

2), their reactions with CH_3CHO lead to $\text{PrOz-}d_0/(\text{PrOz-}d_2 + \text{PrOz-}d_0) < 0.5$. The deviation below 0.5 develops because the in-cage recombination of $\text{D}_2\text{CO} + \text{H}_2\text{COO}$ is favored due to the KSIE for D_2CO .^{10a} This leads to $[\text{D}_2\text{COO}] > [\text{H}_2\text{COO}]$ in reactions with CH_3CHO . If an inverse KSIE also promotes the reactivity of D_2COO (calcd 1) and if $[\text{CH}_3\text{CHO}]$ is low, then the faster reactions that produce EtOz over PrOz lead to $[\text{H}_2\text{COO}] > [\text{D}_2\text{COO}]$ and $\text{PrOz-}d_0 > \text{PrOz-}d_2$. However, as $[\text{CH}_3\text{CHO}]$ increases, the formation of PrOz becomes more competitive with EtOz . In that case more $\text{PrOz-}d_2$ than $\text{PrOz-}d_0$ is produced since a larger proportion of PrOz formation occurs when $[\text{CH}_2\text{OO}]$ and $[\text{CD}_2\text{OO}]$ are more nearly equal.

Acknowledgment. This research was supported by Grant CHE-8005471 from the National Science Foundation.

Registry No. Ethylene, 74-85-1; acetaldehyde, 75-07-0; formaldehyde, 50-00-0; deuterium, 7782-39-0.

Deuterium NMR Study of Organic Molecules Absorbed by Zeolites[†]

R. Eckman* and A. J. Vega

Central Research & Development Department
E. I. du Pont de Nemours & Company, Inc.
Experimental Station, Wilmington, Delaware 19898

Received April 15, 1983

Measurement of deuterium NMR spectra has recently been used to study molecular motion in solids.¹ The deuterium quadrupole interaction usually dominates the nuclear spin internal Hamiltonian so that the powder pattern resonance line shapes obtained can be a critical test for models of molecular motion. Also, the rigid-lattice quadrupole splittings are usually less than a few hundred kilohertz and can be observed by use of the quadrupolar spin echo.² In this communication, the first measurement of deuterium spectra of labeled organic molecules adsorbed within the internal channels of a zeolite molecular sieve is presented. In crystalline zeolites, the organic adsorbate can have highly restricted reorientational motion and slow translational diffusion.³ Observation of the deuterium spectrum offers new and direct information on the dynamics of organic molecules within zeolitic materials.

Deuterium spectra were obtained on a Bruker SXP-100 operating at $\omega_0/2\pi(^2\text{H}) = 13.82$ MHz. The synthetic zeolite ZSM-5 was prepared in the hydrogen form with calcination at 550 °C and outgassed at 400 °C in the NMR tube for several hours under vacuum. Loading of organic molecules was then performed by exposing the tube to the vapors over liquid per-deuterated *p*-xylene so that total absorption was 6.9% (w/w). Adsorption on external surfaces of the zeolite was found to be very small and details will be reported in a forthcoming paper.

The deuterium spectra of the absorbed *p*-xylene are shown in Figure 1. The half-spectra (nonquadrature) from Fourier transformation of the quadrupolar echo decay are illustrated at three temperatures. The striking result is that a broad powder pattern spectrum is obtained at all temperatures indicated. These spectra arise from *p*-xylene molecules with highly restricted reorientational motion within the molecular sieve.

[†] Contribution No. 3229.

(1) (a) Hentschel, D.; Sillescu, H.; Spiess, H. W. *Macromolecules* **1981**, *14*, 1605. (b) Rice, D. M.; Wittebort, R. J.; Griffin, R. G.; Meirovitch, E.; Stimson, E. R.; Meinwald, Y. C.; Freed, J. H.; Scheraga, H. A. *J. Am. Chem. Soc.*, **1981**, *103*, 7707.

(2) Davis, J.; Jeffrey, K.; Bloom, M.; Valic, M.; Higgs, T. *Chem. Phys. Lett.* **1976**, *42*, 390.

(3) Breck, D. W. "Zeolite Molecular Sieves"; Wiley: New York, 1974.

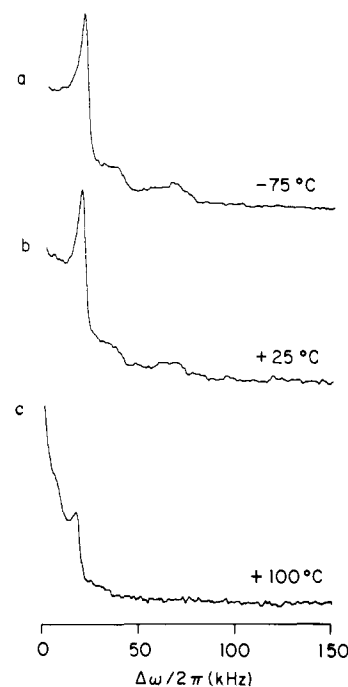


Figure 1. Deuterium NMR spectra of per-deuterated *p*-xylene adsorbed by zeolite ZSM-5. Broad powder pattern spectra due to the deuterium quadrupole interaction are obtained. This results from the restriction of the motion of *p*-xylene by the molecular sieve. The methyl group peak and pedestal are clearly visible having $\omega_Q/2\pi = 35$ kHz. The aromatic site produces a broad, rigid-lattice type spectrum at room temperature and below, having $\omega_Q/2\pi = 124$ kHz. The aromatic powder pattern is motionally narrowed at 100 °C. The vertical scale of c is reduced from that of a and b.

In Figure 1 a and b, the spectra obtained for *p*-xylene are characteristic of rigid-lattice molecular sites found in solids. The symmetric powder pattern arising from the methyl groups is clearly visible and gives $\omega_Q/2\pi = (3/4)e^2qQ = 35$ kHz. We obtain the same value for ω_Q from neat polycrystalline *p*-xylene at -75 °C. A smaller peak that we assign to the *p*-xylene aromatic deuterons appears at larger offset frequency. Taking this as the singular peak in the aromatic deuteron powder pattern gives $\omega_Q/2\pi = 124$ kHz. A sharper peak having about the same relative intensity was obtained for neat polycrystalline *p*-xylene, giving $\omega_Q/2\pi = 126$ kHz.

In Figure 1c, the spectrum of the same sample at +100 °C is shown. The powder pattern of the methyl groups is nearly unchanged. However, the broad component seen at lower temperatures has disappeared and a narrower resonance is found with a shoulder at 8.3-kHz offset. From this spectrum it is apparent that the motion of *p*-xylene molecules is restricted by the molecular sieve even at temperatures approaching those used for commercial reactions.

The spin-lattice relaxation times for the resonance shown in Figure 1 were less than 1 s in all cases. In neat, polycrystalline *p*-xylene the methyl group T_1 , was about 2 s and the aromatic group T_1 was at least 100 s.

From the line-shape and relaxation data, the dynamics of the *p*-xylene reorientation can be investigated. At the high temperature (100 °C), the resonance arising from the aromatic site is evidently motionally narrowed, but the methyl resonance is not. Considering the symmetry of the molecule and the known rotation of the methyl group about its C_3 axis, this can happen if the *p*-xylene molecule can reorient about an axis that passes through the C_3 axes of the para-methyl groups. For the simplest model of free rotation about that axis, a symmetric powder pattern would result for the aromatic site with its singular peak at $\frac{1}{2}[3 \cos^2(60) - 1]124 = 7.8$ kHz. This value is close to the position of the shoulder in Figure 1c. A portion of the narrow resonance at zero offset probably arises from molecules forced out of the zeolite

interior at the high temperature and this overlaps the narrow aromatic resonance. The short T_1 observed for the aromatic site is also due to its reorientation. It is likely that this motion still exists at room temperature and below since the T_1 remains less than 1 s. Also, there appears to be some distortion or flattening of the aromatic resonance line shape (Figure 1b) before the onset of motional narrowing. Investigation of these details is in progress.

We believe that these results provide the first direct spectroscopic evidence of the molecular sieve effect. They demonstrate that deuterium NMR is a useful tool to study the dynamics of molecules within zeolitic materials to shed new light on size and shape phenomena observed in heterogeneous catalysis and other applications of such materials.

Acknowledgment. We are grateful to Dr. Lloyd Abrams for helpful discussions and R. O. Balback for technical assistance.

Registry No. Perdeuterated *p*-xylene, 41051-88-1.

Electrocatalytic Oxidation of Chloride to Chlorine Based on Polypyridine Complexes of Ruthenium

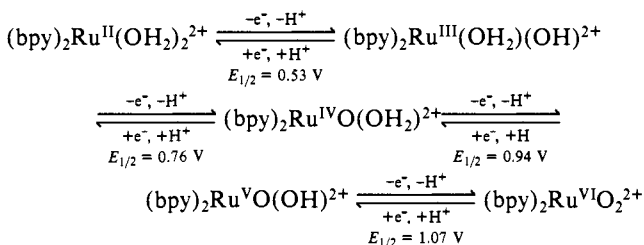
Charles D. Ellis, John A. Gilbert, W. Rorer Murphy, Jr., and Thomas J. Meyer*

Department of Chemistry, The University of North Carolina Chapel Hill, North Carolina 27514

Received April 20, 1983

In recent work, stoichiometric and catalytic oxidations of a series of inorganic and organic substrates by higher oxidation state complexes of ruthenium have been reported.^{1,2} The accessibility of the higher oxidation states is based on a series of closely spaced, coupled proton-electron oxidations of complexes like *cis*-(bpy)₂Ru^{II}(OH₂)₂²⁺ as shown in Scheme I.^{2b}

Scheme I (pH 4.0, vs. SSCE)

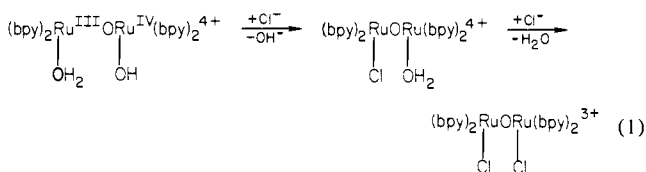


A commercially important electrolytic process is the oxidation of chloride to chlorine at carbon-, or more recently, at RuO₂-impregnated TiO₂ electrodes.³ Possible similarities between complexes like (bpy)₂Ru^{VI}O₂²⁺ and catalytically active RuO₂ surface sites, as well as the successful use of an oxidized form of the dimeric complex, (bpy)₂Ru^{III}(OH₂)ORu^{III}(OH₂)(bpy)₂⁴⁺,^{2a,4} as a catalyst for the oxidation of H₂O to O₂,^{2a} which is also catalyzed by RuO₂, suggested that soluble ruthenium-oxo complexes might also be capable of acting as catalysts for the oxidation of chloride ion to chlorine. We report here that higher oxidation states of the monomeric and dimeric complexes mentioned above

are capable of catalyzing the oxidation of chloride to chlorine at carbon electrodes both with selectivity—preferential oxidation of chloride to chlorine rather than of water to oxygen—and with high thermodynamic efficiency—the catalytic reactions occur with relatively high current densities near the thermodynamic potential for the Cl⁻/Cl₂ couple (+1.13 V vs. SSCE, pH 0–3).⁵

Starting with either (bpy)₂Ru^{II}(OH₂)₂²⁺ or the one-electron oxidized form of the dimer, (bpy)₂(OH₂)Ru^{III}ORu^{IV}(OH)(bpy)₂⁴⁺, oxidation either chemically (using excess Ce(IV)) or electrochemically ($E_{\text{appl}} \geq +1.20$ V) in the presence of chloride results in the generation of chlorine gas as identified by mass spectrometry. In a typical electrocatalytic experiment, electrolysis at a "coarse" (12 holes/linear in.) reticulated vitreous carbon electrode potentiostated at +1.20 V in ca. 30 mL of a 0.05 M HCl solution containing 1.35×10^{-5} mol of [(bpy)₂(OH₂)Ru^{III}ORu^{IV}(OH)(bpy)₂](ClO₄)₅ gave 1.04×10^{-4} mol of chlorine in 132 min. The background current was <12% of the catalyzed current. Chlorine was swept by an argon purge from the working electrode compartment into a cold, aqueous basic solution, and chloride was determined by standard iodometric titration techniques. Comparing the electrochemical stoichiometry as equivalents of electrons passed with moles of chlorine titrated gave a current efficiency of 44% and a turnover number of 7. H₂ was produced at a platinized Pt electrode in the second cell compartment, and the volume of H₂ produced was consistent with the electrochemical current efficiency within experimental error. Blank experiments show that the major loss mechanism in our relatively unsophisticated cell design is the diffusion of chlorine to the cathode compartment. The electrocatalytic reaction is notable, since no significant production of O₂ was observed by gas chromatography. At a glassy carbon disk electrode (geometric area = 0.035 cm²),⁶ current densities of 1.5 mA/cm² were reached (using 10⁻³ M dimer, 0.1 M NaCl, 0.1 M HClO₄) although it should be noted that the actual surface area of the electrode is probably considerably larger than the geometric area, since large surface pits are characteristic of glassy carbon surfaces. Current densities for both the monomer and dimer systems decrease notably after extended electrolysis times.

The results of independent electrochemical, spectral, and chemical isolation studies provide insight into the details of the catalyzed oxidations. The decrease in catalytic current with time is attributed to anation by chloride as shown in eq 1 for the



Ru(III)–Ru(IV) dimer. Neither of the chloride-containing dimers are effective as catalysts for the oxidation of chloride to chlorine.⁶ On the basis of cyclic voltammetry in the absence of chloride, oxidation of the III,III dimer (bpy)₂(OH₂)Ru^{III}ORu^{III}(OH₂)(bpy)₂⁴⁺ to the III,IV dimer (bpy)₂(OH₂)Ru^{III}ORu^{IV}(OH)(bpy)₂⁴⁺ occurs at $E_{1/2} = +0.79$ V (0.1 M HClO₄). Further oxidation of the III,IV dimer in moderately acidic media appears to occur by a two-electron, two-proton step, presumably to give (bpy)₂(OH)Ru^{IV}ORu^VO(bpy)₂⁴⁺, although no information is yet available concerning either structure or an appropriate description of the oxidation state because of the reactivity of the three-electron oxidized dimer. The Ru(IV)–Ru(V) dimer appears to be the reactive component in the catalytic oxidation of Cl⁻ to Cl₂ via the

(1) (a) Moyer, B. A.; Thompson, M. S.; Meyer, T. J. *J. Am. Chem. Soc.* **1980**, *102*, 2310–12. (b) Moyer, B. A.; Sipe, B. K.; Meyer, T. J. *Inorg. Chem.* **1981**, *20*, 1475–80. (c) Thompson, M. S.; Meyer, T. J. *J. Am. Chem. Soc.* **1982**, *104*, 4106. (d) Thompson, M. S.; Meyer, T. J. *Ibid.* **1982**, *104*, 5070.

(2) (a) Gersten, S. W.; Samuels, G. J.; Meyer, T. J. *J. Am. Chem. Soc.* **1982**, *104*, 2049. (b) Takeuchi, K. J.; Samuels, G. J.; Gersten, S. W.; Gilbert, J. A.; Meyer, T. J. *Inorg. Chem.* **1983**, *22*, 1407.

(3) (a) O'Grady, W.; Iwakura, C.; Huang, J.; Yeager, E. In "Electrocatalysis"; Brieter, H. W., Ed.; The Electrochemical Society: Princeton, NJ, 1974. (b) DeNora, O. *Chem. Eng. Tech.* **1970**, *42*, 222; **1971**, *43*, 182. (c) South African Patent 68/7371; 68/7482. German patent 2 021 422, 1969; 2 014 746; 1 915 951, 1970. British patent 1 206 863, 1970.

(4) Weaver, T. R.; Meyer, T. J.; Adeyemi, S. A.; Brown, G. M.; Eckberg, R. P.; Hatfield, W. E.; Johnson, E. C.; Murray, R. W.; Untereker, D. *J. Am. Chem. Soc.* **1975**, *97*, 3039.

(5) All potentials are reported vs. the saturated sodium chloride calomel electrode, which is +0.234 V vs. the normal hydrogen electrode (see: Bard, A. J.; Faulkner, L. R. "Electrochemical Methods"; Wiley: New York, 1980).

(6) The appearance of (bpy)₂ClRuORu(OH₂)(bpy)₂⁴⁺ and (bpy)₂ClRuORuCl(bpy)₂³⁺ can be followed either electrochemically or spectroscopically. For (bpy)₂ClRuORu(OH₂)(bpy)₂⁴⁺ in 0.1 M HClO₄ $E_{1/2} = +0.67$ V, λ_{max} 465 nm, and for (bpy)₂ClRuORuCl(bpy)₂³⁺, $E_{1/2} = +0.54$ V, λ_{max} 470 nm. Note that we are assuming that the dimer (bpy)₂ClRuO(OH₂)(bpy)₂⁴⁺ exists dominantly as the aquo ion in 0.1 M HClO₄ by analogy with (bpy)₂(OH₂)RuORu(OH)(bpy)₂⁴⁺.